Subsurface Energetics of the Gulf Stream near the Charleston Bump

WILLIAM K. DEWAR† AND JOHN M. BANE, JR.*

Marine Sciences Program, University of North Carolina at Chapel Hill, Chapel Hill, NC 27514

(Manuscript received 26 October 1984, in final form 27 June 1985)

ABSTRACT

The energy budgets of the eddies and the mean flow in the Gulf Stream near a topographic feature known as the Charleston bump are computed. First, we consider these results in the context of the amplification hypothesis for the development of Gulf Stream meanders. According to this hypothesis, the finite amplitude Gulf Stream fluctuations observed offshore of Onslow Bay are the result of the destabilizing effect of the bump on the Stream. The present dataset was obtained both immediately upstream and downstream of the bump, and the results of our analysis suggest: 1) Immediately south of the Charleston bump, the eddies perform net work on the Gulf Stream at a rate of $(1.02 \pm .66) \times 10^{-2}$ ergs cm $^{-3}$ s^{-1} by transporting momentum offshore; 2) The net work performed by the eddies south of the bump is not used locally to accelerate the mean; rather, it is exported to the rest of the ocean at a rate of $(1.58 \pm 1.39) \times 10^{-2}$ ergs cm^{-3} s^{-1}; 3) In spite of the net work performed by the eddies south of the bump, eddy kinetic energy apparently does not decrease; 4) Immediately north of the Charleston bump, the flow appears to be both barotropically and baroclinically unstable. These results support the amplification hypothesis by demonstrating the destabilizing effect of the bump on the eddies (points 1 and 4) and that upstream perturbations may survive to encounter the bump topography (point 3). Other results of our analysis are that the release of mean kinetic energy by the eddies constitutes the dominant form of energy conversion and that eddy pressure work may be an important factor in the fluctuation energy budget.

The second application of our calculations is to a characterization of the mean Gulf Stream in the South Atlantic Bight (SAB). The results of this analysis indicate the following: 1) The mean Gulf Stream kinetic energy flux increases downstream at a rate of $(2.17 \pm .98) \times 10^{-2}$ ergs cm^{-3} s^{-1}; 2) The eddies tend to decelerate the mean flow at a rate of $(-0.57 \pm 1.3) \times 10^{-2}$ ergs cm^{-3} s^{-1}; 3) In order that the mean energy equation be balanced, the Gulf Stream in the SAB must be releasing mean potential energy by flowing down a mean pressure gradient. Thus we have evidence suggesting the existence of a component of the pressure gradient associated with the Gulf Stream which is not geostrophically balanced. The downstream pressure gradient inferred at our array site is consistent with published estimates of mean alongshore pressure gradients in the SAB; however, the partitioning of the pressure force between mean acceleration and eddy Reynolds stress most likely holds only near the bump. We also estimate the net loss from the mean potential energy in the SAB using our measured conversion rate and demonstrate that it compares in magnitude but is opposite in sign to that thought to occur downstream of Cape Hatteras. Thus we argue that the Gulf Stream in the SAB is exhibiting some of the properties of the inflow regions of western boundary layers in inviscid inertial models of the general ocean circulation. Our measurements, however, also indicate the presence of vigorous eddies whose effects in the mean energy equation are potentially sizeable. Such eddies are, of course, not contained in strictly inviscid, inertial models of the western boundary layer.

1. Introduction

One of the unanswered questions in physical oceanography concerns the effects of eddies and time-dependent phenomena on the mean circulation of the world ocean. It is not generally known, for example, if the eddies act to maintain or degrade the mean flow through eddy transports of heat and momentum, or if their effects are statistically insignificant. Of particular importance are the interactions of eddies and western boundary currents, primarily because of the role that western boundary currents play in determining the structure of the basin-scale flow. A number of field experiments have recently been conducted in the Gulf Stream along the continental margin of the southeastern United States (see the 30 May 1983 special issue of the *Journal of Geophysical Research* for a collection of related papers). Several of these studies point to a region offshore of Charleston, South Carolina (near the so-called Charleston bump) as a center of dynamic activity, being a point of persistent seaward deflection of the Gulf Stream (Pashinski and Maul, 1973; Brooks and Bane, 1978; Pietrafesa *et al.*, 1978; Legeckis, 1979) and where the lateral meanderings of the Gulf Stream undergo a dramatic 'amplification' (Knauss, 1969; Maul *et al.*, 1978; Bane and Brooks, 1979; Bane, 1983; Hood and Bane, 1983; Olson *et al.*, 1983). In the pres-

† Present address: Department of Oceanography, Florida State University, Tallahassee, FL 32306.

* Also, the Departments of Physics and Geology, UNC, Chapel Hill, N.C. 27514

ent paper, we use data from the Gulf Stream Deflection and Meander Energetics Experiment (DAMEX, Bane and Dewar, 1983) to examine the interactions between the mean Gulf Stream and its fluctuations in the vicinity of the Charleston bump with a view toward defining the energetics of this region.

2. Background

a. Gulf Stream structure in the South Atlantic Bight

The structure of the eddies and the mean flow have been previously studied at certain locations in the South Atlantic Bight (SAB, Fig. 1). For the most part, eddies on the inshore (cyclonic) side of the Gulf Stream perform net work on the mean flow, while those on the offshore (anti-cyclonic) side of the Stream are energized by the mean flow. These results have been confirmed off Miami (Webster, 1961a; Oort, 1964; Schmitz and Niiler, 1969; Brooks and Niiler, 1977), Jacksonville (Webster, 1965; Oort, 1964), at 30°N (Lee and Atkinson, 1983; Lee and Waddell, 1983), and off Onslow Bay (Webster, 1965; Brooks and Bane, 1981, 1983; Hood and Bane, 1983). Thus the effect of eddies on the Gulf Stream in the SAB appears not to be very dependent on downstream location, but to be very dependent on cross-stream location. In spite of that, Schmitz and Niiler (1969) and Brooks and Niiler (1977) have suggested that the net energy conversion from the eddies to the mean when integrated across the Gulf Stream is negligible.

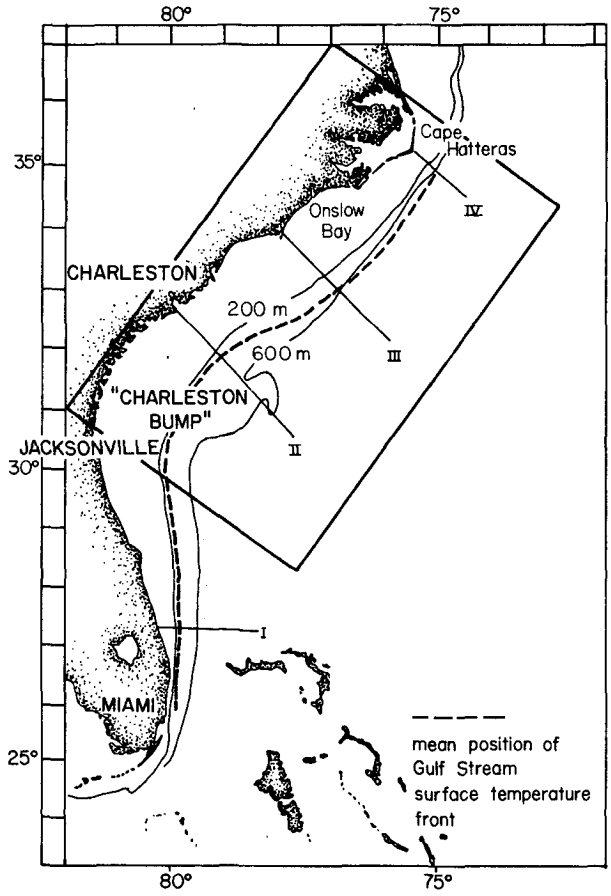

FIG. 1. The continental margin of the eastern United States. The location of the Gulf Stream surface thermal front as determined by Bane and Brooks (1979) and Olson, Brown and Emmerson (1983) is indicated by the dashed line. Also shown are the 200 m and the 600 m isobaths. The perturbation in the 600 m isobath is the Charleston bump, a major topographic feature which is thought to play an important role in the local dynamics of the Gulf Stream. The inset encloses the study area and is shown in greater detail in Fig. 2.

Data on the Gulf Stream in the SAB are also available from satellite observations of the Gulf Stream surface thermal front, which has been shown to indicate the location of the subsurface flow (Olson *et al.*, 1983). According to these data, the lateral variance in the frontal location increases slowly, progressing northward from Florida along the mean Gulf Stream path. At 32°N, eddy growth suddenly and dramatically increases, and lateral meander peak-to-trough amplitudes double within ~40 km. By 33°N, the frontal position variance has begun to decrease, and just downstream from Cape Hatteras the lateral fluctuations of the Gulf Stream are at a local minimum (Maul *et al.*, 1978; Bane and Brooks, 1979; Halliwell and Mooers, 1979; Legeckis, 1979).

b. The amplification hypothesis

One of the interesting features in the structure of the mean Gulf Stream is the sudden growth of lateral fluctuations at 32°N; however, the dynamics governing this phenomenon are as yet unknown. Brooks and Bane (1981, 1983) have suggested that the eddies north of 32°N are primarily low-frequency (~1-week period) Gulf Stream meanders, and that the amplification of the frontal position variance depends partly on meander generation and evolution. Most of the theories about meanders have centered on topographic effects, as the rapid eddy growth commences at the location of the Charleston bump. Examples are the steady state theories of Rooney *et al.* (1978) and Chao and Janowitz (1979), although their application is somewhat limited as current meter (Brooks and Bane, 1983) and satellite data (Maul *et al.*, 1978; Legeckis, 1979; Vukovich and Crissman, 1980) show that meanders are highly time-dependent.

Bane (1983) has offered an explanation for meander structure near the bump in his amplification hypothesis. The instantaneous Gulf Stream can be thought of as a combination of eddies superimposed upon a mean current, in which case significant distortions in the shape of the Gulf Stream can be thought of as large amplitude meanders. According to this hypothesis, such meanders are the result of an instability process, in which perturbations upstream of the bump are amplified as they encounter the bump topography. The hypothesis thus accounts for the occasional eastwardly directed Gulf Stream deflection at the bump (cf. Brooks

and Bane, 1978) as the combination of an unusually large meander and the local seaward deflection of the mean Gulf Stream. Time-dependency of the eddies is explained in terms of an intermittent, upstream generation mechanism. The growth and subsequent decay of the lateral meander amplitudes is argued to be a consequence of the locally weakened topographic constraint at the Charleston bump. A basic assumption of the amplification hypothesis is that the region south of the bump is an area of at best very weak eddy energy loss. If this were not true it is unlikely that a small amplitude perturbation of the Stream could survive until it reached the bump topography.

Evidence in favor of the amplification hypothesis is as follows: 1) Webster (1961a, 1965) and Hood and Bane (1983) demonstrated that downstream of the bump, the meanders are consistently losing energy in their interactions with the mean flow and that the classical meanders are central to this process; 2) Luther and Bane (1985) have computed the mixed instabilities of a Gulf Stream-like jet on the continental margin and found the structure and characteristics of one of the primary modes to agree well with those of the classical meanders; 3) Lee (1981) and Lee and Atkinson (1983) discuss a typical meander-type upstream of the bump (the so-called "Frontal Eddy") whose structure resembles that of the classical meander of Webster (1961b) and Bane *et al.* (1981); and 4) Legeckis (1979), Vukovich and Crissman (1980) and Lee *et al.* (1981) have used satellite SST data to document the growth of an eddy as it passed through the bump region.

The data presented in this paper also support the basic tenets of the amplification hypothesis by demonstrating that upstream perturbations can survive to encounter the bump and that the eddies are organized just north of the bump so as to extract energy from the mean flow.

c. *Eddy structure south of the Charleston bump*

A different scientific point which we consider concerns an apparent disagreement between the satellite and *in situ* data obtained along the U.S. continental margin. The satellite data suggest that eddy variance should increase moving northward from Florida to roughly 33°N (Olson *et al.*, 1983). Historical current meter and hydrographic observations show consistently, however, that the inshore Gulf Stream meanders lose both kinetic and potential energy to the mean flow (Webster, 1961a, 1965; Oort, 1964; Schmitz and Niiler, 1969; Brooks and Niiler, 1977; Hood and Bane, 1983). Our analysis suggests how this seeming paradox may be resolved.

d. *Gulf Stream mean energy*

Although the potential vorticity dynamics of the Gulf Stream are now reasonably well known from a theoretical point of view, a comparable understanding of the constraints on western boundary layer energy is just emerging (Fofonoff, 1981; Fofonoff and Hall, 1983). One of the most model-dependent characteristics of the western boundary energy concerns the release of mean potential energy by flow down a mean pressure gradient in the boundary layer. If the boundary layer is presumed to be frictional, as by Stommel (1948) or Munk (1950), the energy released in this manner is irreversibly lost. The other extreme is represented by the inviscid, inertial model proposed by Fofonoff (1954). The mean potential energy release in this case is used to intensify the mean kinetic energy along the western boundary. Conversely, the flow proceeds up a mean pressure gradient on the eastern basin boundary and the kinetic energy is reconverted to potential energy. It is a general property of inertial general-circulation models that energy is recirculated in this manner.

We suggest that the mean kinetic energy equation requires a potential energy release by flow down a mean pressure gradient in order to be balanced. The inferred energy release occurs at a rate comparable in magnitude but opposite in sign to that which apparently occurs farther downstream (Fofonoff and Hall, 1983); thus, we support the conjecture of Fofonoff (1981) that the Gulf Stream recirculates energy. The force balance as we measure it appears to be local, however, and possible reasons for this are discussed. The recirculation of energy suggests that the Gulf Stream possesses some inertial characteristics. However, eddies also appear to be non-negligible in their effects in the mean energy equation and thus the comparison of the oceanic Gulf Stream with inviscid, inertial models is not immediate. We end by speculating on how the eddies influence the integrated Gulf Stream force balance.

3. The DAMEX Experiment and Data Processing

The field phase of DAMEX took place from September 1981 to April 1982, and consisted of current meter mooring deployments, hydrographic surveys, and AXBT surveys. We shall be primarily concerned with a subset of the current meter data. Fourteen Aanderaa RCM-4 current meters on seven moorings were placed in three locations along the continental margin. The study area is shown in Fig. 2 and details about the moorings are provided in Table 1. Arrays E and F were located immediately upstream and downstream of the Charleston bump, respectively. A single mooring, G, was located off Onslow Bay.

We will discuss the data from arrays E and F. Each consisted of three moorings deployed in an L-shaped configuration (see Fig. 2). Two of the moorings in each array were located on the 400 m isobath and the remaining mooring was located on the 300 m isobath. Two current meters were supported at nominal depths of 210 m and 270 m by each mooring.

The current meters recorded temperature, conductivity, current speed and current direction at 30-minute

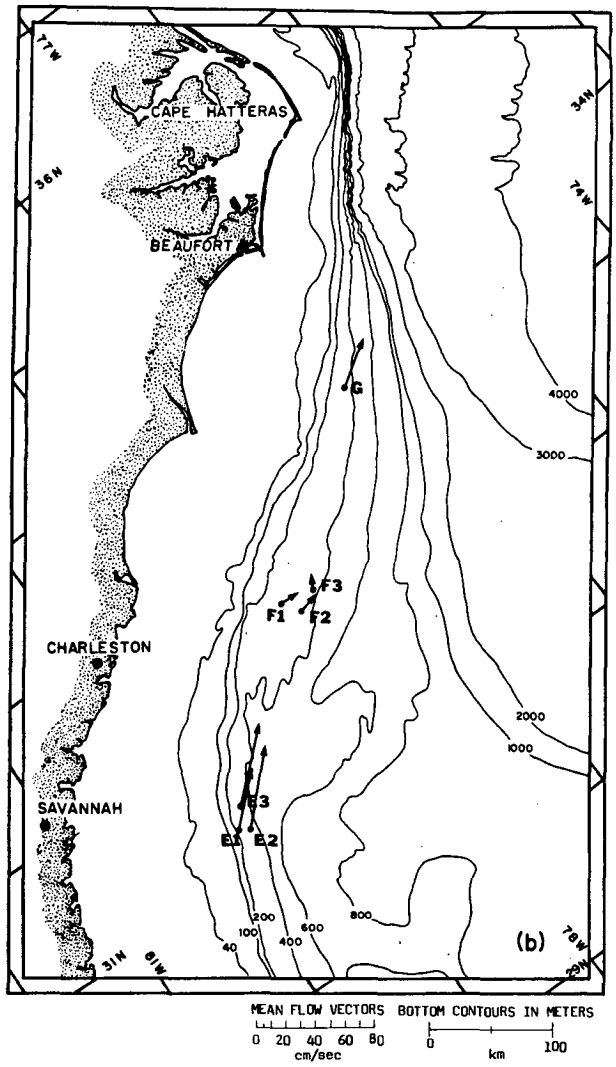

FIG. 2. The study area. The Charleston bump is centered at 31°N, 79°W. The DAMEX experiment employed three arrays, labelled E, F and G in the diagram. Arrays E and F each consisted of three moorings deployed in an L-shaped pattern and were positioned immediately upstream and downstream of the bump. Array G consisted of a lone mooring and was placed off Onslow Bay, the site of an earlier experiment (Brooks and Bane, 1983). The mean flow vectors from the top current meters in array E and the current meters that functioned for the duration of the experiment at F and G are also shown.

intervals. The raw data were low-pass filtered in the manner of Hood and Bane (1983) using a Lanczos-type filter (Brooks, 1976) with a quarter power point at 1 cycle/40 hours and an energy rejection factor of 10^{-6} at 1 cycle/12 hours. The resulting time series had an equivalent sampling interval of 6 hours. Complete documentation of the data, processing methods, and related topics are given by Bane and Dewar (1983).

The energy budgets of both the mean flow and the eddies require estimates of the means and variances of several quantities. The values of such quantities are quite dependent on depth in the DAMEX study area (see Table 2) owing to the strong vertical shear of the Gulf Stream. We have attempted to minimize this effect in our calculations at array E by first computing the required means and variances at each current meter and then linearly interpolating them to a standard depth. Failure of the bottom instrument from one of the E moorings forced us to use the depth of the top meter at that mooring (219 m) as the standard depth.

Linear interpolation in the vertical was not possible at array F owing to short velocity records at a few key current meters. Nonetheless, complete data sets averaging 205 days in length were obtained from at least one meter on each mooring in array F, from which the sign of the most important quantities can be inferred.

One measurement required additional processing. The conductivity probe on the bottom instrument of mooring E2 (see Fig. 2) returned values that were apparently systematically biased. As a result, the inferred salinity and density values were unacceptably low on average, although fluctuations about the mean were reasonable. Thus, we retained the measured value of $\langle \rho'^2 \rangle$ at that meter but discarded the measured value of $\langle \rho \rangle$, where the angle brackets denote a time average. As a consequence, an estimate of the mean vertical density gradient could not be made at this mooring. This problem was solved by using the estimate of the mean vertical density gradient from the nearest mooring, which was 3.9 km away.

Errors for the means and variances have been computed as described in Appendix A. Errors for the linearly interpolated quantities and the terms in the energy equations have been calculated using standard formulae for the sums and products of independent quantities (see for example Bevington, 1969).

4. Results

In this section we discuss and compare the estimates of the terms in the eddy and mean energy equations. We assume throughout that the Boussinesq equations apply. We briefly mention the derivations of the equations; complete analyses are given by Brooks and Niiler (1977) and Szabo and Weatherly (1979). A physical discussion of the equations is given by Bryden (1983).

An analysis of the energy equations using current meter data is of necessity incomplete, as not all the terms in the equations can be estimated. In particular, we have no direct measurements of vertical velocity nor reliable measurements of pressure at a fixed depth. Thus, it must be borne in mind when estimates are presented in the following section that some terms have been omitted. For example, our estimate of the divergence of eddy kinetic-energy flux does not include vertical advection. Other instances where such omissions occur should be apparent.

The full eddy kinetic- and potential-energy equations involve triple correlations. We have found the values

TABLE 1. Mooring data.

Array	Number	Location	Deployment (1981)	Recovery (1982)	Meter	Number	Depth (m)
E	1	31 14.7°N, 79 40.7°W	19 Sep	25 Apr	T	5705	201
					B	3424	261
E	2	31 13.8°N, 79 38.5°W	19 Sep	25 Apr	T	5707	229
					B	5708	289
E	3	31 24.7°N, 79 33.7°W	19 Sep	25 Apr	T	5706	219
					B	3427	279
F*	1	32 25.5°N, 78 15.3°W	18 Sep	22 Apr	T	3337	206
					B	3423	266
F*	2	32 16.9°N, 78 10.4°W	18 Sep	22 Apr	T	3425	210†
					B	3344	270†
F	3	32 22.3°N, 77 55.7°W	18 Sep	22 Apr	T	3426	212
					B	3345	272
G	—	33 21.0°N, 76 40.7°W	17 Sep	21 Apr	T	3332	210†
					B	3343	270†

distance E1 − E2 = 3.86 km
distance E2 − E3 = 21.58 km
distance E1 − E3 = 21.59 km
distance F1 − F2 = 17.69 km
distance F2 − F3 = 25.10 km
distance F1 − F3 = 31.24 km
distance E2 − F1 = 165 km
distance F2 − G = 183 km
distance E2 − G = 354 km

* These moorings supported a bottom pressure gauge.
† Nominal depths used.

of these terms to be both small compared to other terms in the equations and statistically insignificant. We therefore will not consider them explicitly in the following analysis.

A number of means and covariances are involved in the following equations. Estimates of these quantities obtained from the current meters at array E are listed in Table 2. The values of these quantities interpolated to the standard depth (219 m) are given in Table 3. Estimates of processes (e.g., barotropic release of eddy kinetic energy) at the standard depth are listed in Table 4.

a. Eddy kinetic energy at array E

The eddy kinetic-energy equation is obtained by subtracting the ensemble averaged ($\langle \cdot \rangle$) momentum equations from the total momentum equations, vector multiplying the residuals by the fluctuating velocity ($\underline{u}'$), and ensemble-averaging. Thus:

$$\frac{\partial}{\partial x_j}(\langle u_j \rangle \langle u_i'^2 \rangle/2)$$

$$= -\frac{\partial}{\partial x_j}\langle p' u_j' \rangle - \langle u_i' u_j' \rangle \frac{\partial}{\partial x_j}\langle u_i \rangle - g\langle w' \rho' \rangle. \quad (1)$$

Primed variables are eddy variables, p is pressure, w vertical velocity and g gravity; ρ' is nondimensional, and defined by:

$$\rho' = (\rho_T - \rho_0)/\rho_0$$

where ρ_T is the total density and ρ_0 a reference density. We have used the summation convention with indices i and j running from 1 to 3. $(x_1, x_2, x_3) = (x, y, z)$ are the cross-slope, alongslope and vertical coordinates, and $(u_1, u_2, u_3) = (u, v, w)$ are the cross-slope, alongslope and vertical velocities. Equation 1 relates the divergence of mean flux of eddy energy to the divergence of eddy pressure work, the conversion of mean kinetic energy, and the eddy work against gravity.

The standard interpretation of the quantity $-\langle u_i' u_j' \rangle \partial/\partial x_j \langle u_i \rangle$ is as a measure of barotropic instability. The largest contribution at E to this quantity is $-\langle u'v' \rangle \partial/\partial x \langle v \rangle$ (see Table 4). Its value is negative and larger than its error; thus, we infer that the meanders are passing northward momentum from the weak inshore flow toward the high-velocity core of the Gulf Stream. This requires the meander velocity components to be positively correlated, as the cross-slope gradient of $\langle v \rangle$ is positive. Positive (negative) alongslope perturbation velocities must therefore correspond to positive (negative) cross-slope perturbation velocities.

TABLE 2. Statistics at array E.*

	$\langle u \rangle$	$\langle v \rangle$	$\langle u'v' \rangle$	$\langle u'u' \rangle$	$\langle v'v' \rangle$	$\langle u'E' \rangle^a$	$\langle v'E' \rangle^a$	$\langle \sigma_t \rangle^b$	$\langle u'\rho' \rangle$	$\langle v'\rho' \rangle$	$\langle \rho'^2 \rangle$	$\left\langle u' \frac{\rho'^2}{2} \right\rangle$	$\left\langle v' \frac{\rho'^2}{2} \right\rangle$	d
E1T	8.90	41.6	249.9	81.5	1135	1485	2885	26.96	$0.966e^{-4}$	$-0.118e^{-2}$	$0.81e^{-7}$	$0.102e^{-7}$	$-0.701e^{-7}$	201
	1.5	5.4	53.1	13.1	225	2177	9563	0.061	$2.53e^{-4}$	$0.104e^{-2}$	$0.13e^{-7}$	$0.51e^{-7}$	$1.7e^{-7}$	
E1B	1.73	18.7	33.4	19.4	361	140	−1494	27.31	$0.126e^{-3}$	$0.262e^{-3}$	$0.353e^{-7}$	$0.333e^{-8}$	$0.327e^{-7}$	261
	0.66	3.3	9.0	2.0	82.9	172	1871	0.05	$0.089e^{-3}$	$0.45e^{-3}$	$0.158e^{-7}$	$1.3e^{-8}$	$0.68e^{-7}$	
E2T	8.75	58.6	160.	54.6	984	1063	3945	26.81	$-9.05e^{-5}$	$-1.34e^{-3}$	$0.447e^{-7}$	$0.442e^{-8}$	$-0.552e^{-8}$	229
	0.98	5.2	26.5	7.2	184	1359	7943	0.043	$0.124e^{-3}$	$0.608e^{-3}$	$0.260e^{-7}$	$2.e^{-8}$	$7.60e^{-8}$	
E2B	9.53	42.8	99.5	78.3	352	140	−1364	—	$-0.920e^{-3}$	$-0.729e^{-3}$	$0.923e^{-7}$	$0.304e^{-6}$	$0.264e^{-6}$	289
	1.60	2.7	18.8	16.9	90	543	1973		$0.51e^{-3}$	$0.49e^{-3}$	$0.641e^{-7}$	$0.306e^{-6}$	$0.241e^{-6}$	
E3T	10.5	56.9	209.	43.6	1368	−1487	−8162	26.80	$0.828e^{-4}$	$0.650e^{-3}$	$0.467e^{-7}$	$-0.174e^{-7}$	$-0.939e^{-7}$	219
	1.2	7.4	71.	14.5	341	2369	13130	0.049	$1.53e^{-4}$	$0.898e^{-3}$	$0.207e^{-7}$	$0.209e^{-7}$	$1.34e^{-7}$	
E3B	—	—	—	—	—	—	—	27.28	—	—		$0.277e^{-7}$		279
								0.046				$0.120e^{-7}$		

* The top number in each bin is the estimate for that statistic. The bottom number is its error. All velocities are in cm s^{-1} and densities in gm cm^{-3}. The notation "e" followed by a superscripted integer signifies 10 raised to that integer power. The depth of each instrument in meters is given in the last column.

[a] $E' = (u'^2 + v'^2)/2$.

[b] σ_t = sigma-t = $(\rho_T - 1) \times 1000$.

Sample data from E are shown in Fig. 3 which exhibit this behavior.

The sum of the eddy–mean flow interaction terms

$$-\langle u_i' u_j' \rangle \frac{\partial}{\partial x_i} \langle u_j \rangle = (-1.02 \pm .66) \times 10^{-2} \text{ ergs cm}^{-3} \text{ s}^{-1}$$

is also negative and significantly different from zero. This suggests that on average the eddies just south of the Charleston bump are releasing kinetic energy in their interactions with the mean flow.

A compact way of describing eddies is by their characteristic ellipse, which is determined by the eddy velocity variance in both horizontal directions and the covariance of the velocity components. Pedlosky (1979) and Brooks and Bane (1983) have shown how the positive (negative) orientation of this ellipse with respect to the mean shear signals eddy acceleration (deceleration) of the mean. The angle with respect to the local isobaths of both the major axes of the eddy ellipses and the directions of the mean flow measured at E are listed in Table 4 and illustrated in Fig. 4. Note that the eddies at the two southernmost moorings appear to lean with the shear, indicating an energizing of the mean by the eddies. The ellipse at the most northern E mooring, however, is oriented against the mean flow, suggesting the eddies there obtain kinetic energy from the mean. The net transfer over the array is dominated by the two southern moorings and results in the above negative energy conversion rate. The geographical variability in the eddy ellipses is interesting as the northern mooring is closer to the Charleston bump.

The other estimable quantity in Eq. 1 is the divergence of the mean flux of eddy energy. The largest contribution to this quantity comes from the cross-slope advection of northward eddy energy and is significantly greater than zero (see Table 4). The total divergence:

$$\frac{\partial}{\partial x_j} (\langle u_j \rangle \langle u_i'^2 \rangle)/2 = (0.67 \pm 0.70) \times 10^{-2} \text{ ergs cm}^{-3} \text{ s}^{-1}$$

is not significantly different from zero; however, its estimated value is positive. This would imply a gain in eddy kinetic energy in the downstream direction, but the uncertainty of the estimate is too large to claim that convincing evidence has been found.

The above estimates suggest that the eddies upstream of the Charleston bump are configured so as to perform work on the mean flow and that the energy loss from the eddies necessary to perform this work does not result in a reduction in eddy kinetic-energy flux. Rather, some other source drives the work on the mean flow, and may also be weakly energizing the eddies. At the least, the preceding quantities are not balanced—their residual:

TABLE 3. Standard depth statistics at array E.[a]

	$\langle u\rangle$	$\langle v\rangle$	$\langle u'v'\rangle$	$\langle u'u'\rangle$	$\langle v'v'\rangle$	$\langle u'E'\rangle$[b]	$\langle v'E'\rangle$[b]	$\langle\sigma_t\rangle$[c]	$\langle u'\rho'\rangle$	$\langle v'\rho'\rangle$	$\langle\rho'^2\rangle$	$\left\langle u'\frac{\rho'^2}{2}\right\rangle$	$\left\langle v'\frac{\rho'^2}{2}\right\rangle$
$E1_s$	6.8	34.7	185	62.9	903	1082	1571	27.07	$0.105e^{-3}$	$-0.747e^{-3}$	$0.672e^{-7}$	$0.814e^{-8}$	$-0.589e^{-7}$
	1.0	3.9	37	9.2	160	1525	6717	0.045	$0.18e^{-3}$	$0.74e^{-3}$	$0.10e^{-7}$	$3.60e^{-8}$	$1.2e^{-7}$
$E2_s$	8.6	61.3	170	50.7	1090	1216	4830	26.75	$0.478e^{-4}$	$-1.45e^{-3}$	$0.367e^{-7}$	$-0.455e^{-7}$	$-0.504e^{-7}$
	1.2	6.1	31	8.8	216	1590	9272	0.052	$1.7e^{-4}$	$7.1e^{-4}$	$0.430e^{-7}$	$0.56e^{-7}$	$0.97e^{-7}$
$E3_s$	10.5	56.9	209	43.6	1368	−1487	−8162	26.80	$0.828e^{-4}$	$0.650e^{-3}$	$0.467e^{-7}$	$-0.174e^{-7}$	$-0.939e^{-7}$
	1.2	7.4	71	14.5	341	2370	13135	0.049	$1.5e^{-4}$	$0.9e^{-3}$	$0.210e^{-7}$	$0.21e^{-7}$	$1.34e^{-7}$

[a] As in Table 2, except all statistics have been interpolated to 219 m.
[b] $E' = (u'^2 + v'^2)/2$.
[c] σ_t = sigma-t = $(\rho - 1) \times 1000$.

TABLE 4. Energy calculations at array E.

1. eddy work against the mean shear:

$$-\langle u'u'\rangle \frac{\partial}{\partial x}\langle u\rangle - \langle u'v'\rangle\left[\frac{\partial}{\partial y}\langle u\rangle + \frac{\partial}{\partial x}\langle v\rangle\right] - \langle v'v'\rangle \frac{\partial}{\partial y}\langle v\rangle$$

$$= (-0.275 \pm 0.235) \times 10^{-3} + (-0.167 \pm 0.153) \times 10^{-3} + (-1.22 \pm 0.37) \times 10^{-2} + (0.248 \pm 0.547) \times 10^{-2} = -(1.02 \pm 0.66) \times 10^{-2}$$

2. divergence of mean flux of eddy energy:

$$\frac{\partial}{\partial x}\langle u\rangle\langle u'^2\rangle\Big/2 + \frac{\partial}{\partial x}\langle u\rangle\langle v'^2\rangle\Big/2 + \frac{\partial}{\partial y}\langle v\rangle\langle u'^2\rangle\Big/2 + \frac{\partial}{\partial y}\langle v\rangle\langle v'^2\rangle\Big/2$$

$$= (0.157 \pm 1.72) \times 10^{-4} + (0.426 \pm 0.347) \times 10^{-2} + (-0.145 \pm 0.251) \times 10^{-3} + (0.257 \pm 0.61) \times 10^{-2} = (0.67 \pm 0.70) \times 10^{-2}$$

3. eddy-potential-energy conversion: (g = 980 cm/sec^2)

$$g\langle u'\rho'\rangle \frac{\partial}{\partial x}\langle\rho\rangle\Big/\left(\frac{\partial}{\partial z}\langle\rho\rangle\right) + g\langle v'\rho'\rangle \frac{\partial}{\partial y}\langle\rho\rangle\Big/\left(\frac{\partial}{\partial z}\langle\rho\rangle\right) = (0.106 \pm 0.175) \times 10^{-2} + (0.133 \pm 0.269) \times 10^{-3} = (1.20 \pm 1.73) \times 10^{-3}$$

4. divergence of mean eddy-potential-energy flux: (g = 980 cm/sec^2)

$$-\frac{\partial}{\partial x} g\langle u\rangle\langle\rho'^2\rangle\Big/\left(2\frac{\partial}{\partial z}\langle\rho\rangle\right) - \frac{\partial}{\partial y} g\langle v\rangle\langle\rho'^2\rangle\Big/\left(2\frac{\partial}{\partial z}\langle\rho\rangle\right) = (-0.3 \pm 0.88) \times 10^{-2} + (-0.121 \pm 1.11) \times 10^{-2} = (-0.42 \pm 1.4) \times 10^{-2}$$

5. eddy acceleration of the mean flow:

$$-\langle u\rangle \frac{\partial}{\partial x}\langle u'u'\rangle - \langle v\rangle \frac{\partial}{\partial x}\langle u'v'\rangle - \langle u\rangle \frac{\partial}{\partial y}\langle u'v'\rangle - \langle v\rangle \frac{\partial}{\partial y}\langle v'v'\rangle$$

$$= (0.24 \pm 0.25) \times 10^{-3} + (0.19 \pm 0.60) \times 10^{-2} + (-0.17 \pm 0.34) \times 10^{-3} + (-0.76 \pm 1.1) \times 10^{-2} = (-0.57 \pm 1.25) \times 10^{-2}$$

6. divergence of the mean flux of mean kinetic energy:

$$\frac{\partial}{\partial x}\langle u\rangle\langle u\rangle^2\Big/2 + \frac{\partial}{\partial x}\langle u\rangle\langle v\rangle^2\Big/2 + \frac{\partial}{\partial y}\langle v\rangle\langle u\rangle^2\Big/2 + \frac{\partial}{\partial y}\langle v\rangle\langle v\rangle^2\Big/2$$

$$= (0.43 \pm 0.13) \times 10^{-3} + (0.31 \pm 0.06) \times 10^{-1} + (0.40 \pm 0.22) \times 10^{-3} + (-0.10 \pm 0.076) \times 10^{-1} = (2.17 \pm 0.98) \times 10^{-2}$$

7. export of eddy energy:

$$\frac{\partial}{\partial x}\langle u\rangle\langle u'u'\rangle + \frac{\partial}{\partial x}\langle v\rangle\langle u'v'\rangle + \frac{\partial}{\partial y}\langle u\rangle\langle u'v'\rangle + \frac{\partial}{\partial y}\langle v\rangle\langle v'v'\rangle$$

$$= (0.32 \pm 3.4) \times 10^{-4} + (0.10 \pm 0.068) \times 10^{-1} + (0.34 \pm 0.40) \times 10^{-3} + (0.052 \pm 0.12) \times 10^{-1} = (1.58 \pm 1.39) \times 10^{-2}$$

8. orientations of mean flow, characteristic eddy ellipses and mass fluxes:

$\theta_{\text{mean flow}} = \tan^{-1}[\langle u\rangle/\langle v\rangle]$,	$\theta_{\text{ellipse}} = 0.5\tan^{-1}[2\langle u'v'\rangle/(\langle u'u'\rangle - \langle v'v'\rangle)]$,	$\theta_{\text{mass flux}} = \tan^{-1}[\langle u'\rho'\rangle/\langle v'\rho'\rangle]$
E1: $\theta_{\text{mean flow}} = -11.0°$	$\theta_{\text{ellipse}} = -11.9°$	$\theta_{\text{mass flux}} = 278°$
E2: $\theta_{\text{mean flow}} = -8.0°$	$\theta_{\text{ellipse}} = -9.0°$	$\theta_{\text{mass flux}} = 272°$
E3: $\theta_{\text{mean flow}} = -10.5°$	$\theta_{\text{ellipse}} = -8.8°$	$\theta_{\text{mass flux}} = -7.3°$

Angles are measured relative to the along-topography direction. All other estimates are in ergs cm^{-3} s^{-1}.

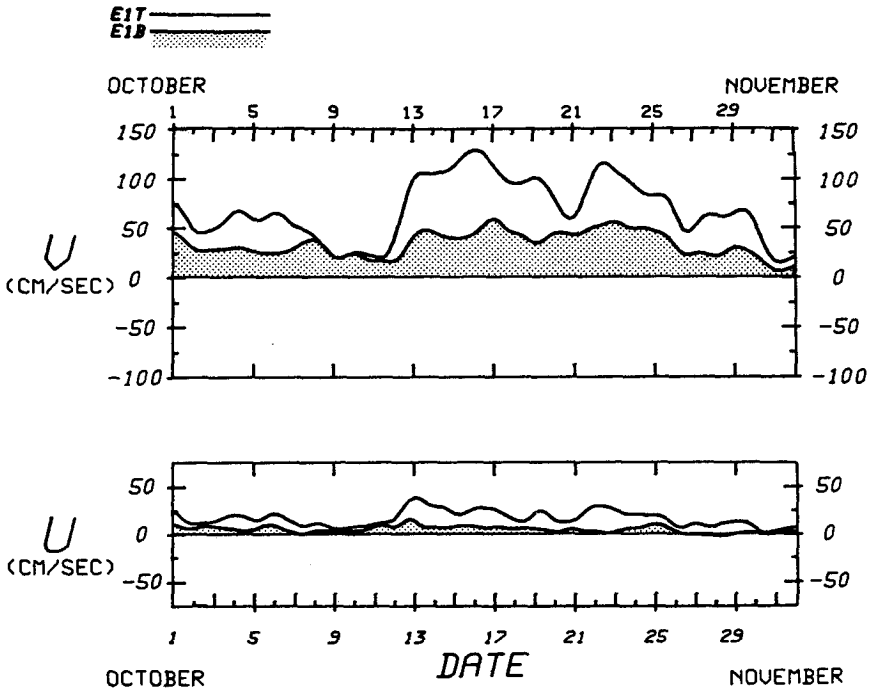

FIG. 3. Meanders at array E. The shaded data are from the bottom instrument. Note the perturbation U and V (across and along topography) velocities agree in sign over most of the wave periods, consistent with a net offshore momentum flux.

$$\frac{\partial}{\partial x_j}(\langle u_j\rangle\langle u_i'^2\rangle)/2 + \langle u_i'u_j'\rangle\frac{\partial}{\partial x_i}\langle u_j\rangle = (1.69 \pm .96) \times 10^{-2} \text{ ergs cm}^{-3}\text{ s}^{-1}$$

is significantly different from zero. It is therefore necessary that eddy pressure work, vertical eddy momentum fluxes, or the eddy release of potential energy be active in order that the energy equation be balanced. We are unable to comment directly on the first two of these processes, although the second is probably small (cf. Brooks and Niiler, 1977). The latter process is considered in the next subsection.

b. *Eddy potential energy at array E*

The equation governing eddy potential energy is obtained by subtracting the ensemble-averaged density equation from the total density equation, multiplying the residual by ρ', and ensemble averaging. The result is:

$$-\frac{\partial}{\partial x_j}[g\langle u_j\rangle\langle\rho'^2\rangle/(2\partial\langle\rho\rangle/\partial z)] = g\langle\rho'u_\alpha'\rangle\,\partial\langle\rho\rangle/\partial x_\alpha/(\partial\langle\rho\rangle/\partial z) + g\langle w'\rho'\rangle - [g\langle u_j\rangle\langle\rho'^2\rangle/2][\partial^2\langle\rho\rangle/\partial x_j\partial z]/(\partial\langle\rho\rangle\partial z)^2 \quad (2)$$

where α runs from 1 to 2. The above equation relates the divergence of the mean flux of eddy potential energy to the release of mean available potential energy by the eddies and a correction due to variations in the local mean stratification.

The usual interpretation of the quantity

$$[g\langle\rho'u_\alpha'\rangle\partial/\partial x_\alpha\langle\rho\rangle]/(\partial\langle\rho\rangle/\partial z)$$

is as a measure of baroclinic instability. Neither of the terms in this quantity is estimated to be larger than its error; therefore, their sum:

$$g\langle u_\alpha'\rho'\rangle\frac{\partial}{\partial x_\alpha}\langle\rho\rangle\Big/(\partial\langle\rho\rangle/\partial z) = (0.12 \pm .17) \times 10^{-2} \text{ ergs cm}^{-3}\text{ s}^{-1}$$

is not significantly different from zero (see Table 4). Bane and Dewar (1986) found that the deeper temperature fluctuations lagged the shallower temperature fluctuations at array E and thus that the fluid did not appear to be baroclinically unstable. We are unable here to detect a measurable eddy release of mean potential energy, which supports their conclusion. Finally, note that the above estimate is an order of magnitude smaller than the estimate of the eddy release of mean kinetic energy.

The other quantity we can estimate in Eq. 2 is the divergence of the mean flux of eddy potential energy. Here, also, neither term in the estimate is larger than its error and, therefore, neither is their sum:

$$-\frac{\partial}{\partial x_\alpha}[g\langle u_\alpha\rangle\langle\rho'^2\rangle/(2\partial\langle\rho\rangle/\partial z)] = (-0.42 \pm 1.4) \times 10^{-2} \text{ ergs cm}^{-3}\text{ s}^{-1}.$$

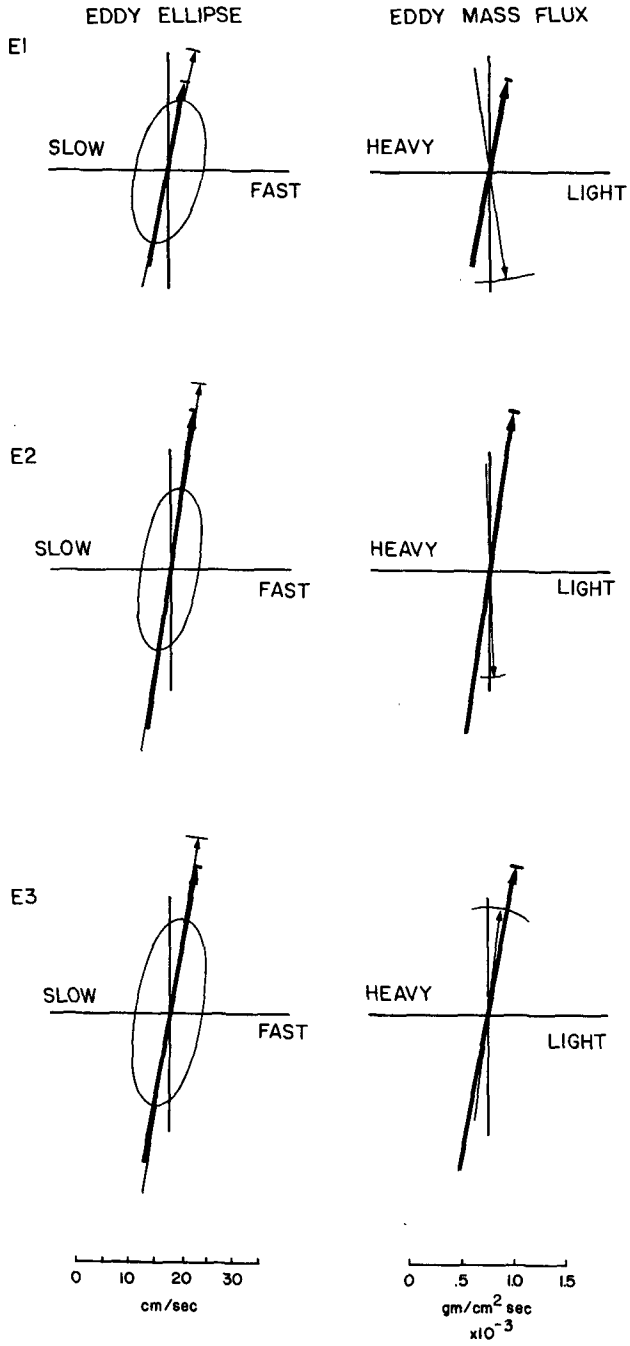

FIG. 4. Eddy ellipses and mass fluxes at array E. The $x(y)$ axis is oriented offshore (alongshore) as determined by the local topography. The bold arrow is in the direction of the mean flow. We assume slow (fast) flow and heavy (light) water is located inshore (offshore) of the mean flow. The eddy ellipse is sketched in the first column and the direction of the eddy mass flux is shown by the lighter arrow in the second column. The arcs indicate plus or minus one standard deviation for the orientations.

This estimate is negative and suggests, except for the error, an overall loss of eddy potential energy.

In summary, we are unable to conclude much about eddy potential energy conversion or flux divergence at array E, except perhaps that eddy potential-energy conversion is substantially weaker than eddy kinetic-energy conversion. This is nonetheless a useful result and is discussed further in the next subsection.

c. *Total eddy energy at array E*

The sum of Eqs. (1) and (2) returns the total eddy energy equation:

$$\frac{\partial}{\partial x_j}[\langle u_j\rangle\langle u_i'^2\rangle/2 - g\langle u_j\rangle\langle \rho'^2\rangle/(2\partial\langle\rho\rangle/\partial z)]$$

$$= -\langle u_i'u_j'\rangle\frac{\partial}{\partial x_i}\langle u_j\rangle + g\langle u_\alpha'\rho'\rangle(\partial\langle\rho\rangle/\partial x_\alpha)/(\partial\langle\rho\rangle/\partial z)$$

$$- g\langle u_j\rangle\langle\rho'^2\rangle/[2(\partial\langle\rho\rangle/\partial z)^2]\frac{\partial^2\langle\rho\rangle}{\partial x_i\partial z} - \frac{\partial}{\partial x_i}\langle p'u_i'\rangle \quad (3)$$

where the interpretation of the terms is as before. Note that the eddy work against gravity, $g\langle w'\rho'\rangle$, has dropped out.

The mean total energy-flux divergence:

$$\frac{\partial}{\partial x_j}[\langle u_j\rangle\langle u_i'^2\rangle/2 - g\langle u_j\rangle\langle\rho'^2\rangle/(2\partial\langle\rho\rangle/\partial z)]$$

$$= (0.25 \pm 1.5)\times 10^{-2}\ \text{ergs cm}^{-3}\ \text{s}^{-1}$$

is relatively small and not significantly different from zero (see Table 4); thus, we are unable to measure a net change in the net eddy kinetic plus potential energy flux at array E. The sum of the barotropic and baroclinic conversion terms is, however, significantly different from zero and negative:

$$g\langle u_\alpha'\rho'\rangle(\partial\langle\rho\rangle/\partial x_\alpha)/(\partial\langle\rho\rangle/\partial z) - \langle u_i'u_j'\rangle\frac{\partial}{\partial x_j}\langle u_i\rangle$$

$$= (-0.90 \pm .67)\times 10^{-2}\ \text{ergs cm}^{-3}\ \text{s}^{-1}.$$

The largest contribution to the above comes from the eddy release of mean kinetic energy.

It is interesting to speculate on how the total eddy-energy equation is balanced. The residual of the estimated total eddy-energy flux and the eddy–mean flow energy conversions:

$$(1.15 \pm 1.6)\times 10^{-2}\ \text{ergs cm}^{-3}\ \text{s}^{-1}$$

is not different from zero. It is, however, arguable that the residual is actually positive, as the most likely value for the eddy-energy flux divergence is small and of the wrong sign to balance the eddy–mean flow energy conversion terms. Thus, it is possible that one of the quantities we have not measured, i.e., pressure work or one involving vertical velocity, is an important, active part of the total eddy-energy equation. Brooks and Niiler (1977) have commented on the potential importance of eddy pressure work. This is a possibility which our analysis also admits.

Note that our measurements are consistent both with the satellite indications that eddy variance in the SAB

grows in the downstream direction and the subsurface measurements of eddy energy release obtained elsewhere. These data suggest the balance we have inferred at array E might well hold over much of the SAB.

d. Mean kinetic energy at array E

The final equation we will consider is that governing mean kinetic energy, and is obtained by ensemble-averaging the horizontal momentum equations and forming the scalar product of the result with the ensemble-averaged horizontal velocity:

$$\frac{\partial}{\partial x_j}\langle u_j\rangle\langle u_\alpha\rangle^2\Big/2 = \frac{-\partial}{\partial x_\alpha}\langle p\rangle\langle u_\alpha\rangle - \langle u_\alpha\rangle\frac{\partial}{\partial x_i}\langle u'_\alpha u'_i\rangle \quad (4)$$

where subscripts α obtain the values 1 and 2 only. Equation 4 relates the divergence of the mean flux of kinetic energy to mean pressure work and the eddy acceleration of the mean flow. Mean potential energy enters implicitly in Eq. 4 through pressure work.

The individual terms involved in the mean flow acceleration by the eddies are at best marginally significant (see Table 4). Their sum

$$-\langle u_\alpha\rangle\frac{\partial}{\partial x_i}\langle u'_\alpha u'_i\rangle = [-0.57 \pm 1.3]\times 10^{-2}\ \text{ergs cm}^{-3}\ \text{s}^{-1}$$

is therefore not significantly different from zero and indicates no measurable eddy effect on the mean. It is worth remarking, however, that the sign of the measured quantity is negative and would otherwise indicate an eddy deceleration of the mean.

The largest contribution to divergence of the mean advection of mean kinetic energy comes, somewhat surprisingly, from cross-stream advection and is significantly greater than zero. The total divergence:

$$\frac{\partial}{\partial x_j}\langle u_j\rangle\langle u_\alpha\rangle^2\Big/2 = [2.17 \pm .98]\times 10^{-2}\ \text{ergs cm}^{-3}\ \text{s}^{-1}$$

is also significantly positive and is the largest of any estimate we have computed. The above value indicates that more kinetic energy is leaving a control volume surrounding array E than is entering it, or that the mean flow is gaining kinetic energy in the downstream direction.

The two quantities we have estimated from Eq. 4 are not balanced; indeed the residual of the above terms:

$$\frac{\partial}{\partial x_j}\langle u_j\rangle\langle u_\alpha\rangle^2\Big/2 + \langle u_\alpha\rangle\frac{\partial}{\partial x_j}\langle u'_\alpha u'_j\rangle = (2.74 \pm 1.7)\times 10^{-2}\ \text{ergs cm}^{-3}\ \text{s}^{-1}$$

is significantly greater than zero. Accordingly, the mean flow is gaining in kinetic energy but apparently not at the expense of the eddies, whose most likely effect is to decelerate the flow. The other sources of mean kinetic energy are acceleration by vertical eddy stress, vertical advection of kinetic energy and pressure work. Of these, the most likely candidate for the source is mean pressure work. Scaling arguments in support of this statement will be reviewed later; we mention here that a balance including pressure work requires a downstream drop in pressure. This is interesting for two reasons. First, downstream pressure gradients are characteristic of inertial Gulf Stream models (Fofonoff, 1962). Second, this result suggests that the mean Gulf Stream flow and the mean Gulf Stream pressure gradient are not perpendicular and thus that we have inferred a deviation from geostrophy in the Gulf Stream mean structure.

e. Export of eddy energy at array E

We are then left with somewhat of a paradox. The earlier analysis of the eddy kinetic-energy equation showed that the eddies are configured so as to transfer energy to the mean, but the analysis of the mean kinetic-energy equation suggests that the eddies are acting as a mean energy sink. These apparently contradictory results are resolved by recognizing that the eddy source for the mean energy differs from the eddy sink for the eddy energy. These quantities differ by the divergence of a vector:

$$\frac{\partial}{\partial x_j}\langle u_i\rangle\langle u'_i u'_j\rangle$$

which is perhaps most easily understood as the "export" of eddy energy (Bryden, 1983).

The largest terms in this equation involve the divergence of the downstream mean transport of eddy variance. The sum of all components is significantly greater than zero (see Table 4):

$$\frac{\partial}{\partial x_j}\langle u_i\rangle\langle u'_i u'_j\rangle = [1.58 \pm 1.39]\times 10^{-2}\ \text{ergs cm}^{-3}\ \text{s}^{-1}.$$

Its positive value suggests that eddy variance is being removed from the region by mean advection.

Thus, the eddies and the mean flow interact so as to release both eddy and mean flow kinetic energy, but that energy is not used locally. Rather it is exported and can eventually become either mean or eddy energy. Furthermore, as our measurements are unable to detect a significant change in the local eddy energy and also suggest an increase in mean kinetic energy, the net energy being exported must be supplied by other sources. Likely candidates are the mean and eddy pressure work, although we have no measurements to substantiate directly these conjectures.

f. Array F

A shortage of data at array F prevented us from interpolating the means and variances required by Eqs.

(1)–(4) to a standard depth. Therefore we cannot estimate accurately the flux divergences, the conversion rates, or the statistical significance of any of the processes. We can, however, obtain an estimate of the sign of the baroclinic and barotropic conversion terms by computing the angle of the eddy momentum and mass fluxes relative to the mean momentum and density gradients. If the eddy momentum transports are pointed down the mean momentum gradient, the eddies are organized so as to gain kinetic energy from the mean (Pedlosky, 1979; Bryden, 1983). We will take this as an indication of barotropic instability. If eddy mass transports are pointed down the mean density gradient, the eddies are releasing potential energy from the mean (Pedlosky, 1979; Bryden, 1983). We will take this as an indication of baroclinic instability. Given eddy mass and momentum flux measurements at F, we will estimate the conversion rates using the mean gradients measured upstream at E. It is not our intention that these numbers be taken literally; rather, they should be interpreted as order of magnitude estimates only. We feel that the signs so inferred for the energy conversions are reasonable.

The means and covariances computed from the data at F are listed in Table 5. We have extracted the eddy-ellipse orientations from the data and also the orientation of the mean flow and eddy mass fluxes. These are given in Table 6. It is reasonable to assume that both the mean shear and mean density gradient are perpendicular to the mean flow and that lower (higher) momentum (density) is found inshore of the instruments.

One of the two southern F moorings was located on the 300 m isobath and the other on the 400 m isobath. The top (bottom) meter operated on the inshore (offshore) mooring. The eddy momentum flux measured at the inshore meter is directed onshore away from the more rapid mean flows, as indicated by the orientation of the eddy ellipse in Fig. 5. The primary contribution to eddy kinetic-energy conversion at E came from the quantity:

$$\langle u'v' \rangle \frac{\partial}{\partial x} \langle v \rangle$$

or, the cross-stream transport of downstream momentum multiplied by the cross-stream mean shear. The value of the appropriate component of the momentum flux relative to the mean flow at the inshore F meter is obtained by rotating the data in Table 5 from the frame aligned with the local topography to one aligned with the local mean flow. The cross-stream eddy transport of downstream eddy momentum is thus

$$\langle u'v' \rangle = -226.75 \text{ cm}^2 \text{ s}^{-2}$$

and is comparable to the fluxes at E. The negative sign denotes an onshore momentum flux. Assuming a cross-stream $\langle v \rangle$ gradient at F comparable to that at E, the

TABLE 5. Statistics at array F.*

	$\langle u \rangle$	$\langle v \rangle$	$\langle u'v' \rangle$	$\langle u'u' \rangle$	$\langle v'v' \rangle$	$\langle u'E' \rangle$[a]	$\langle v'E' \rangle$[a]	$\langle \sigma_t \rangle$[b]	$\langle u'\rho' \rangle$	$\langle v'\rho' \rangle$	$\langle \rho^2 \rangle$	$\left\langle u' \frac{\rho^2}{2} \right\rangle$	$\left\langle v' \frac{\rho^2}{2} \right\rangle$
F1T	10.8	8.25	298	353	617	5659	8523	27.11	0.215e^{-2}	0.934e^{-3}	0.433e^{-7}	0.441e^{-8}	0.268e^{-6}
	3.79	4.46	70.9	78.5	101	3827	5419	0.059	0.081e^{-2}	0.764e^{-3}	0.220e^{-7}	0.188e^{-6}	0.174e^{-6}
F2B	8.80	12.14	253	372	519	2948	4152	27.19	−0.16e^{-2}	−0.271e^{-2}	0.154e^{-5}	0.339e^{-5}	0.775e^{-5}
	3.73	4.84	59.0	80.3	62.0	3204	3890	0.089	0.19e^{-2}	0.27e^{-2}	0.104e^{-5}	0.529e^{-5}	0.762e^{-5}
F3B	−0.49	12.4	172	293	670	1645	5985	27.17	0.104e^{-2}	−0.67e^{-3}	0.304e^{-7}	−0.131e^{-6}	0.203e^{-6}
	2.08	5.18	45.7	64.0	114	2630	4680	0.036	0.040e^{-2}	0.611e^{-3}	0.173e^{-7}	0.107e^{-6}	0.187e^{-6}

* The top number in each bin is the estimate for that statistic. The bottom number is its error. All velocities are in cm s^{-1} and densities in gm cm^{-3}. The notation "e" followed by a superscripted integer signifies 10 raised to that integer power.

[a] $E' = (u^2 + v^2)/2$.

[b] σ_t = sigma-t = $(\rho_T - 1) \times 1000$.

TABLE 6. Orientations of mean flow, eddy momentum fluxes, and eddy mass fluxes at F.*

	$\theta_{\text{mean flow}} = \tan^{-1}[\langle u\rangle/\langle v\rangle]$	$\theta_{\text{ellipse}} = \frac{1}{2}\tan^{-1}[2\langle u'v'\rangle/(\langle u'^2\rangle - \langle v'^2\rangle)]$	$\theta_{\text{mass flux}} = \tan^{-1}\left[\frac{\langle u'\rho'\rangle}{\langle v'\rho'\rangle}\right]$
F1T:	$= -52.6°$,	$= -33.08°$,	$= -66.5°$
F2B:	$= -35.9°$,	$= -36.7°$,	$= 149.3°$
F3B:	$= 2.3°$,	$= -21.2°$,	$= 122.9°$

* All angles are measured relative to an axis lying along the local topography.

above is consistent with a net mean-to-eddies energy conversion of

$$-\langle u'v'\rangle \frac{\partial}{\partial x}\langle v\rangle = 1.55 \times 10^{-2} \text{ ergs cm}^{-3}\text{ s}^{-1}$$

where we have not calculated an error because of the obvious shortcomings of the estimate. Nonetheless, this value is of the magnitude of the upstream estimates, and the sign agrees with that inferred from the eddy ellipses.

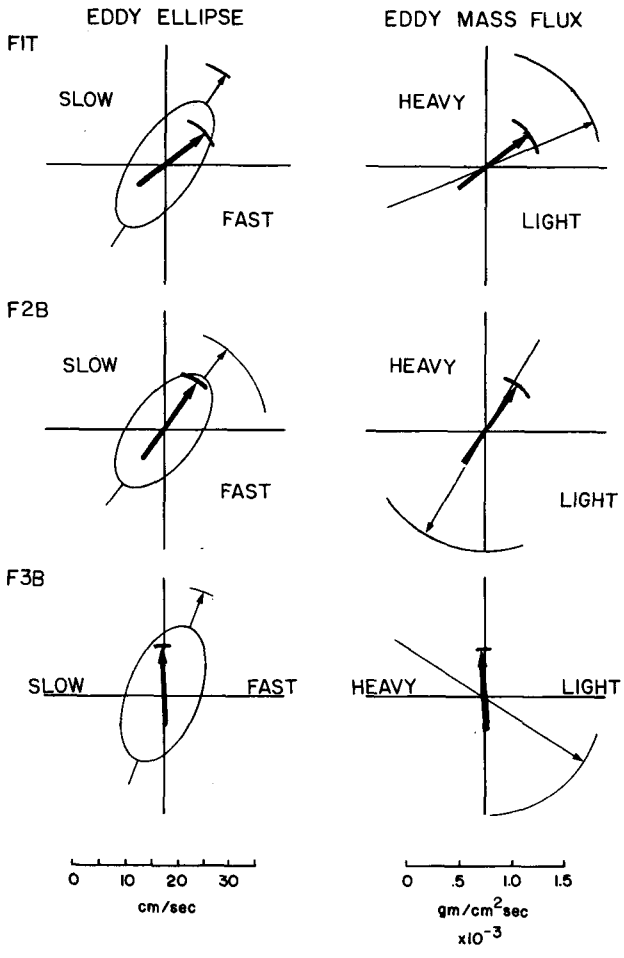

FIG. 5. As in Fig. 4 except data is from array F.

The eddy mass flux at the inshore F meter is directed toward light water and suggests baroclinically unstable flow. The component of flux parallel to the assumed mean density gradient is

$$\langle u'\rho'\rangle = 0.57 \times 10^{-3} \text{ gm cm}^{-2}\text{ s}^{-1}$$

and is much larger in magnitude than the along-gradient eddy mass fluxes at E. Assuming mean density gradients comparable to those measured at E, the estimated baroclinic conversion rate becomes roughly

$$g\langle u'\rho'\rangle(\partial\langle\rho\rangle/\partial x)/(\partial\langle\rho\rangle/\partial z) = 0.78 \times 10^{-2} \text{ ergs cm}^{-3}\text{ s}^{-1}$$

which is several times those measured at E. Again we have not computed errors.

Both barotropic and baroclinic conversion estimates suggest an energizing of the eddies by mean flow instabilities. Also, the baroclinic estimates are comparable in magnitude to the barotropic estimates at F, which strongly contrasts with the situation at E.

The eddy ellipse at the offshore southern mooring (F2B in Fig. 5) appears to be leaning with the mean shear, although the difference in orientation is only 2°. This suggests that the eddy release of mean kinetic energy is possibly insignificant. The magnitude of the eddy momentum flux in the direction of the assumed mean momentum gradient is

$$\langle u'v'\rangle = -17.67 \text{ cm}^2\text{ s}^{-2}$$

and is substantially smaller than the momentum flux estimates at E and at the inshore F mooring. The approximate energy conversion rate (using the mean cross-slope momentum gradient at E) is

$$-\langle u'v'\rangle \frac{\partial}{\partial x}\langle v\rangle = 0.12 \times 10^{-2} \text{ ergs cm}^{-3}\text{ s}^{-1}$$

which, although positive, is one order of magnitude smaller than comparable estimates at E. It is doubtful if this number is significantly positive. Its small value and the small angle of the eddy ellipse relative to the mean flow probably reflect a negligible energy conversion.

The temperature and conductivity sensors at F2B appeared to malfunction intermittently for short intervals; thus, the error in the estimated eddy mass flux there is probably overwhelming. We have nonetheless

computed the relevant quantities at the offshore mooring. Accordingly, the component of eddy mass flux parallel to the mean density gradient is

$$\langle u'\rho' \rangle = 0.27 \times 10^{-3} \text{ gm cm}^{-2} \text{ s}^{-1}$$

which is relatively small and reflects the slight angle between the eddy mass flux and the direction of the mean flow. The magnitude of the associated baroclinic conversion estimate (using the mean density gradient from E) is

$$\langle u'\rho' \rangle \frac{\partial}{\partial x} \langle \rho \rangle \Big/ (\partial \langle \rho \rangle / \partial z) = 0.374 \times 10^{-2} \text{ ergs cm}^{-3} \text{ s}^{-1}$$

which is comparable to the statistically insignificant values measured at E. The magnitudes of both energy conversion estimates at F2B suggest that the local conversions are small and insignificant. This is in marked contrast with the situation at the inshore mooring.

The bottom instrument on the northernmost F mooring operated properly for the duration of the experiment. The eddy momentum fluxes at that instrument were oriented against the mean shear (see Fig. 5). The eddy momentum-flux component in the direction normal to the mean flow was directed offshore at a magnitude of

$$\langle u'v' \rangle = 184 \text{ cm}^2 \text{ s}^{-2}$$

which is comparable to but of opposite sign than the flux at the inshore F mooring. The approximate eddy kinetic-energy conversion is thus roughly

$$-\langle u'v' \rangle \frac{\partial}{\partial x} \langle v \rangle = -1.26 \times 10^{-2} \text{ ergs cm}^{-3} \text{ s}^{-1}$$

which is as large as the conversion rates noted at E and suggests that the downstream eddies at F are releasing eddy kinetic energy to the mean flow by transporting momentum offshore.

Eddy mass flux at the northern F mooring was also directed offshore, from high to low densities, and is thus suggestive of baroclinic instability. The component of mass flux parallel to the assumed mean gradient is

$$\langle u'\rho' \rangle = 1.0 \times 10^{-3} \text{ gm/(cm}^2 \text{ s)}$$

and corresponds to an approximate conversion rate of

$$\langle u'\rho' \rangle \frac{\partial}{\partial x} \langle \rho \rangle \Big/ (\partial \langle \rho \rangle / \partial z) = 1.38 \times 10^{-2} \text{ ergs cm}^{-3} \text{ s}^{-1}$$

which is as large as any of the present eddy-energy conversion estimates. The positive value of this is probably large enough to be significant and indicates a transfer of energy to the eddies by release of mean potential energy.

Thus, the eddies at F give every indication of being substantially different from those at E 180 km upstream. Perhaps the most pronounced difference is the strong indication that eddies are releasing mean potential energy at F. The error involved in the conversion estimates could easily be a factor of 2; nonetheless, the magnitudes of the baroclinic energy conversions are potentially much greater at F than at E. The barotropic energy conversions appear to feed energy to the eddies close to the bump, but change quickly to convert eddy kinetic energy to the mean flow farther downstream. This sudden change is interesting and suggestive of a local effect of the topography. The same tendency for the eddies to energize the mean flow presumably occurs in the eddy potential-energy balance farther downstream. Although we have not measured it here, Hood and Bane (1983) have measured a net exchange of potential energy from the eddies to the mean flow off Onslow Bay.

5. Discussion

It is interesting to place these results within the context of the amplification hypothesis for eddy development near the Charleston bump. Our analysis supports the hypothesis, although it does so in an unexpected manner. With respect to the hypothesis, the potentially damaging discovery was made that the eddies were releasing eddy energy to the mean flow upstream of the bump. This result agrees with similar findings in the SAB by Webster (1961a, 1965) and Lee and Atkinson (1983). One might think that this disproves the amplification hypothesis; however, further analysis revealed no firm evidence for a decrease in the mean flux of eddy energy. In fact, indications were that the mean flux of eddy energy increased downstream a slight amount. The latter result softens the former so that it does not detract from the basic idea behind the amplification hypothesis, which in its barest form requires only that the perturbations do not decay prior to encountering the bump topography. This is consistent with the discovery by Bane and Dewar (1986) that the 2–5 day fluctuations were coherent at arrays E and G at a lag of 9 days. We also have found evidence that the mean flow immediately downstream of the bump is both baroclinically and barotropically unstable. This result indicates that the bump not only has a considerable effect on the Stream, but that the area downstream of the bump is one where eddies may obtain energy directly from the mean, and "amplify."

Nonetheless we do recommend a restatement of the amplification hypothesis based on our findings. We present in Fig. 6 an updated version of a diagram which was given originally by Hood and Bane (1983, their Fig. 2) and which is indicative of the decidedly complicated energy structure of the eddy field. The uppermost part of the diagram is a graph of the SST frontal position variance of the Gulf Stream along the continental margin as measured by satellites. These data suggest weak growth in eddy energy south of the Charleston bump, and rapid growth followed by rapid decay in eddy energy immediately north of the

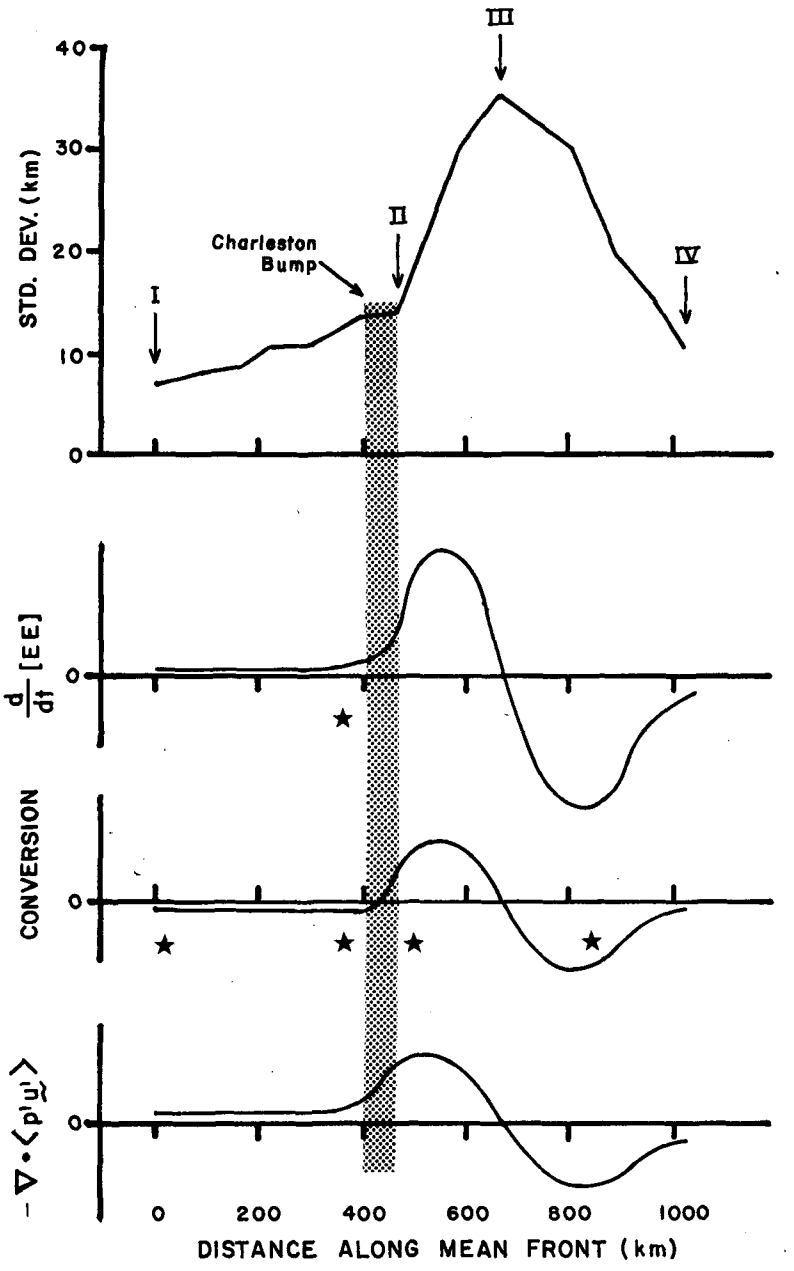

FIG. 6. Schematic of the amplification hypothesis. The above is an amended version of a diagram which was first given by Hood and Bane (1983). Stars show where data have been obtained to verify this picture. The Roman numerals I–IV correspond to the sections indicated in Fig. 1. The top graph is the standard deviation of SST frontal position along the mean Gulf Stream path as measured by satellites. The second graph is a schematic of the time rate of change of eddy energy following a mean fluid parcel [$d(EE)/dt$] as suggested by the top graph. The bottom two graphs are of the sources of eddy energy, i.e. eddy–mean flow interaction (labelled as 'conversion') and eddy pressure work. These latter two sum to give $d(EE)/dt$. The position of the Charleston bump is indicated by the shading.

Charleston bump. Immediately below this graph, we sketch a plot of the time rate of change following a fluid parcel of total eddy energy as would be inferred from the satellite data. South of the bump, the rate is estimated to be very small but slightly positive. The star indicates the one available direct measure of this quantity which we have obtained from array E. The value measured there was slightly positive, in agreement

with the satellite data, although the error bars are large. Immediately north of the bump, the rate is estimated to be significantly positive, consistent with the sudden growth in frontal position variance. Farther downstream, the rate is estimated to be negative, as is indicated by the rapid decline in the frontal position variance. The third graph is of the net eddy-energy gain caused by interactions between the mean flow and the eddies. South of the bump, this effect releases eddy energy and hence is negative in value. Again, the stars indicate where data (historical and DAMEX) support this conjecture. The energy conversion appears to become positive just downstream of the bump. The evidence for this was discussed in this paper and comes from the signature of barotropic and baroclinic energy release from the mean flow inferred from the data at array F. Farther north of the bump, the energy conversions as sketched are consistent with a release of total eddy energy. Such a state was suggested by the most northern F mooring and was somewhat more convincingly demonstrated off Onslow Bay by Hood and Bane (1983). The bottom graph in Fig. 6 is an estimate of the net eddy pressure work along the continental margin. It is important to note that we have no direct measure of this effect and that these rates are inferred as residuals in the eddy energy equation. Accordingly, the eddy pressure work south of the bump is assumed to be positive and slightly greater in magnitude than the eddy release of energy due to eddy–mean flow interaction. The sum of these two effects is slightly positive and is consistent with the satellite measurements of eddy variance. We have indicated an enhanced positive eddy pressure work in the downstream vicinity of the bump, which subsequently switches to a negative eddy pressure work farther downstream. The evidence for this downstream structure comes indirectly from the satellite data; however, the graph suffers from the lack of reliable rate measurements in the eddy-energy equations. As it stands, Fig. 6 suggests that eddy pressure work combines with eddy–mean flow interaction to produce the observed rise and fall in eddy variance downstream of the bump.

Figure 6 is a "straw man" diagram which we offer for two reasons. First, it provides a hypothesis which additional measurements can test. Second, and it is this point which is perhaps the most believable aspect of the diagram, it portrays the complexity involved in the overall energetic structure of the eddy field in the Gulf Stream. The balances in Fig. 6 are consistent with the available data, but the rates are not well known and the geographical coverage is sparse. Further measurements are necessary to support or refute the eddy-energy structure we have suggested here.

Several questions regarding the dynamics of this region of the Gulf Stream remain open. In the simplest eddy–mean flow interaction, eddy energy is directly governed by energy conversion from the mean. An example is the quasi-geostrophic linear instability of a zonal jet (Pedlosky, 1979) in which the eddies grow by feeding on mean kinetic or potential energy. Rather than this simple picture, our data suggest that the net energy released by the interactions of the eddies and the mean flow is exported and neither the mean-flow kinetic energy nor the eddy total energy is locally reduced. Granted, the zonal jet model is time-dependent which contrasts with our analysis in a presumably stationary eddy field, and eddy energy budgets in theoretical calculations are usually integrated as compared to our pointwise estimates. It still appears that an understanding of how energy is distributed geographically in the Gulf Stream by eddy pressure work and export is required. Little has been said about either effect in quasi-geostrophic and shallow water eddy-resolving models, although both may easily be inferred. An exception is the regional energy analysis of eddy-resolving general circulation models conducted by Harrison (1979). Even so, the regions he considered are still orders of magnitude too large and a comparison of his results with ours is not very revealing. We are unaware of any models, numerical or otherwise, that at first glance look promising enough to compare in detail with our data. The best general circulation models have not yet produced any reasonable looking activity on the continental margin. Published simulations using regional models also seem to be missing some important structure (perhaps because of the boundary conditions or the lack of imposed downstream pressure gradients).

The measured net export of energy at array E is an interesting result but is apparently not confined to western boundary currents. Bryden (1983) has reported a similar finding in the mid-ocean; his value of export was approximately 10^{-4} ergs cm^{-3} s^{-1} and is roughly two orders of magnitude smaller than ours. Data from earlier experiments along the continental margin have not been used to estimate export or to balance eddy energy flux divergence against conversion rates, so there is no literature to aid in speculation about the ultimate fate of the exported energy. It would be interesting to analyze the earlier data with these objectives in mind. These considerations are of particular interest with respect to the Gulf Stream mean kinetic-energy balance, as we will point out shortly.

It is of interest to compute effective eddy viscosities and diffusivities for the Gulf Stream as such quantities comment tellingly on the possibilities for simple eddy closures in general circulation models. Also, such information is important to the prediction of the Gulf Stream. The eddy viscosity at array E at the standard depth of 219 m is computed to be:

$$A = -2\langle u'v'\rangle \Big/ \left(\frac{\partial}{\partial x}\langle v\rangle + \frac{\partial}{\partial y}\langle u\rangle\right) = -5.3 \times 10^6 \text{ cm}^2 \text{ s}^{-1}.$$

A comparable value in the Gulf Stream off Florida has

been reported by Lee and Atkinson (1983). The negative value of A is a result of the eddy efforts to accelerate the mean flow and indicates that the eddies might play an important role in maintaining the mean structure. The eddy density diffusivity computed by Array E is not significantly different from zero, which agrees with the observation that the flow is baroclinically stable. We are unable to compute the Austauch coefficients at F; however, indications are that, at the southern moorings at least, both the eddy viscosity and density diffusivity will be positive. This sudden change in the eddy structure (occurring over a separation of 180 km) supports the contention that the Charleston bump is a major influence on the Gulf Stream.

The dominant energy conversion between eddies and mean flow at array E is of a barotropic nature. For example, at E the estimates of the release of eddy kinetic energy to the mean flow are the only ones which we have shown to be significant and are an order-of-magnitude greater than the baroclinic conversion estimates. This result is potentially useful to modelers, as the apparent dominance of barotropic effects might be used as a test for judging the relevance of individual models.

The DAMEX data provide a useful supplement to the growing SAB dataset. Arrays E and F complement the inshore moorings discussed by Lee and Atkinson (1983) and the offshore moorings discussed by Lee and Waddell (1983). One interesting global ramification of the SAB data concerns the "standard" form of Gulf Stream inshore eddies and how that form responds to the perturbation due to the Charleston bump. All indications are that the Gulf Stream inshore meanders in the SAB effect an offshore momentum flux, except in the immediate, downstream vicinity of the bump. The rapid relaxation of the eddy field back to this state (within 100 km downstream of the bump) indicates that the drive to the "standard" configuration is indeed strong. The possibility that eddy pressure work provides a balance in the eddy kinetic-energy equation also suggests that non-local eddy energy sources exist. Thus, it is not clear at present how the eddy field on the inshore Gulf Stream edge is maintained. Further theoretical work on eddy–strong current interaction is necessary to clarify these issues.

Finally, it is interesting to consider the character of the mean flow at array E. The reader is again reminded that our energy analyses suffer from a lack of direct observations of w, so the following discussion is somewhat speculative. Nonetheless, there is a common theme which appears to emerge. Our data suggest a gain in mean kinetic-energy flux and an apparent imbalance of mean energy-flux divergence and eddy–mean flow interaction. Thus we have inferred that other mean kinetic-energy sources, namely vertical advection, vertical eddy Reynolds stress or pressure work, must be important. Unfortunately, we have no measurements that allow us to compute the vertical eddy stress. It is also difficult to estimate the magnitude of this term as it depends critically upon the vertical structure of the covariance of vertical and horizontal velocity, a topic about which little is known. In what follows, we will (perhaps wrongly) neglect vertical eddy stress. Our analysis does suggest that mean vertical kinetic-energy advection needs some consideration. The evidence for this includes the presence of less dense water at the standard depth at the downstream E mooring and the general tendency of the mean flow to cross isobaths from shallower to deeper waters. Thus our measurements appear to be consistent with a slight downward velocity, which is possibly topographically induced. The mean flow at E is directed primarily from the mooring on the 300 m isobath to the downstream mooring on the 400 m isobath over a separation of roughly 22 km. An estimate of the topographically induced downwelling is therefore:

$$\mathbf{u}_B \cdot \nabla h = -.045 \text{ cm s}^{-1}$$

where we have extrapolated the observed mean velocities to the bottom. An order-of-magnitude estimate of the effects of vertical energy advection is thus:

$$\frac{\partial}{\partial z}\langle w\rangle\left(\frac{\langle u\rangle^2}{2}+\frac{\langle v\rangle^2}{2}\right) \approx -10^{-2} \text{ ergs cm}^{-3} \text{ s}^{-1}$$

where we have used the average of the vertical gradients of mean kinetic energy measured at array E. Although comparable in magnitude to the directly measured quantities, this is insufficient to provide a balance in Eq. (4). We are left with a residual of:

$$[1.74 \pm 1.7] \times 10^{-2} \text{ ergs cm}^{-3} \text{ s}^{-1}$$

which, without a careful error analysis, appears to be significantly greater than zero, and suggests that a balance in Eq. (4) requires net positive pressure work. This corresponds in physical terms to a release of mean potential energy caused by a mean flow down a pressure gradient.

It is possible to estimate the magnitude of the required downstream pressure drop from the above residual:

$$-\langle p\rangle_y \approx -\langle v\rangle^{-1}(1.74 \pm 1.7) \times 10^{-2} \text{ ergs cm}^{-3} \text{ s}^{-1}$$
$$= (3 \pm 2.8) \times 10^{-4} \text{ gm cm}^{-2} \text{ s}^{-2}.$$

If vertical energy advection is not included, the pressure-gradient estimate is

$$-\langle p\rangle_y = (4.5 \pm 2.8) \times 10^{-4} \text{ gm cm}^{-2} \text{ s}^{-2}.$$

Using a combination of hydrographic and surface-velocity data, Sturges (1974) has estimated the downstream pressure gradient in the Gulf Stream to be from 2.0 to 2.5 ($\times 10^{-4}$ gm cm^{-2} s^{-2}). This range of values agrees rather well with our former estimate and is within the error bars of our latter estimate.

The "trading" of potential and kinetic energy, such as we have inferred, via pressure work in boundary

currents is a characteristic feature of inertial Gulf Stream models (Fofonoff 1962, 1981); thus, our observations are consistent with the premise that the Gulf Stream is an inertial jet. One implication of this is that the Gulf Stream is recirculating energy. Downstream of Cape Hatteras, Fofonoff and Hall (1983) have suggested that the observed decrease in mean momentum flux in the downstream direction is balanced by an increase in pressure. The resulting flow up the mean pressure gradient is thought to reduce the mean kinetic energy of the Gulf Stream by roughly 50×10^9 J s^{-1}. If we assume that our lower estimate of mean potential-energy release is typical of the Gulf Stream along the continental margin, an estimate of the total Gulf Stream potential-energy loss in the SAB is roughly 70×10^9 J s^{-1}, where we have assumed the conversion occurs in a 1000-km long core region one Rossby deformation radius (50 km) wide by 800 m deep. This potential energy loss is clearly comparable to the gain computed by Fofonoff and Hall (1983). Admittedly, we have applied a point estimate all along the SAB; but this is consistent with the result of Sturges (1974) who observed a pressure drop on the inshore edge of the Gulf Stream along the entire southeastern continental margin.

Sturges (1974) also considered the possible dynamical balances within the downstream momentum equation given his estimated pressure force. He determined that the eddy Reynolds stresses measured off Florida by Schmitz and Niiler (1969) provided a downstream momentum balance. It is of interest to compare the force balance inferred from our measurements with those of Sturges (1974). In the direction of the mean flow, the momentum equation reduces to

$$\langle v\rangle\langle v\rangle_y + \langle w\rangle\langle v\rangle_z = -\langle p\rangle_y - \langle u'v'\rangle_x - \langle v'v'\rangle_y - \langle w'v'\rangle_z.$$

Note that this equation applies to a component of the mean velocity vector, and therefore direct estimates of the terms from our data are sensitive to small errors in the estimation of mean flow direction. The balance inferred by Sturges (1974) involved the first two terms on the right-hand side of the above equation. The balance inferred from our data involves the first term on the left-hand side and the third term on the right-hand side as well. Our inferred pressure force is consistent with a downstream mean flow acceleration of

$$\langle v\rangle\langle v\rangle_y \approx 3 \times 10^{-4} \text{ gm cm}^{-2} \text{ s}^{-2}.$$

Integration demonstrates that this balance cannot describe the Gulf Stream over much of its extent, for accelerations of this magnitude over distances of a few hundred kilometers result in velocities of more than 200 cm s^{-1}. Flows of this speed are not characteristic of the mean subsurface Gulf Stream. While the observed potential energy release and inferred pressure gradient appear to be characteristic of the Gulf Stream in the SAB, the particular partitioning of the pressure force observed at array E does not. The obvious candidate for producing this local balance is the Charleston bump. Although the offshore deflection of the mean Gulf Stream path begins to the north of array E, it is known that the Gulf Stream formed a large relatively stationary offshore arc during the DAMEX experiment (Bane and Dewar, 1986). It is felt that the arc formed as a result of the interaction of the Stream with the bump and its effects were observed at E for roughly three months of the 7-month mooring period. It is possible that our measured force balance reflects this structure.

The observational premise that argues against the generality of our momentum balance at E is that the mean flow speeds are not observed to increase in magnitude along the Gulf Stream's track (Schmitz and Niiler, 1969). What is observed, however, is that the Gulf Stream transport increases appreciably between Florida and Cape Hatteras, with an attendant broadening of the current. Therefore, some mechanism must exist for accelerating newly entrained water from a state of near rest to the observed O(100 cm s^{-1}) velocities typical of the Gulf Stream. Given that the force balance proposed by Sturges (1974) is in our opinion more typical of the Gulf Stream inshore edge, it is interesting to speculate on how the acceleration might occur. We have demonstrated that the inshore edge of the Gulf Stream is a region of export of eddy energy. One possible area to which that energy might be exported is the offshore edge of the Stream. The data reported by Schmitz and Niiler (1969) suggest that both eddy and mean fields in the Gulf Stream anticyclonic zone are obtaining energy in their interactions with each other, and therefore that this must be a region of energy import. A crude estimate of eddy acceleration of the mean from Fig. 1 of Schmitz and Niiler (1968) along with their published estimates of kinetic energy transfer to the eddies (both on the Gulf Stream offshore edge) returns a value of

$$\frac{\partial}{\partial x_j}\langle u_i\rangle\langle u_i'u_j'\rangle \approx -1 \times 10^{-2} \text{ ergs cm}^{-3} \text{ s}^{-1}$$

which is opposite in sign but similar in magnitude to the export we have measured at array E. In the view of Schmitz and Niiler (1969), the net energy transfer to the eddies over the width of the Gulf Stream is negligible; hence, the eddies act primarily to redistribute energy and momentum internally. It is therefore possible that the energy necessary to accelerate the entrained water in the Gulf Stream is released initially by mean pressure work, and distributed laterally by eddies.

Data from several experiments at a variety of locations in the SAB are now available. The primary objectives of the data analyses to date have centered on the time-dependent flow. It would be interesting to compare the character of the mean flow at the other

sites with that inferred here. On the anticyclonic shear side of the Stream, the sign and magnitude of the export of eddy energy are of particular interest. Are the eddies and mean flow in this region importing energy or are they exporting energy as occurs inshore? Also of interest are a number of questions that can be addressed with any of the SAB datasets. Can a net pressure work and net downstream pressure gradient be inferred elsewhere in the SAB and is there a local divergence of the mean flux of mean kinetic energy? How is the pressure force partitioned between mean flow acceleration and eddy stress?

It appears that the mean Gulf Stream structure involves a complicated interplay between mean and time-dependent flow. Among other things, we have taken a few tentative steps in the description of the mean flow dynamics in this paper. It seems advisable to analyze mean Gulf Stream structure elsewhere in the SAB using data already in hand. Such information will undoubtably be valuable and would aid in the understanding of the Gulf Stream system.

Acknowledgments. We gratefully acknowledge the support for this research, which was provided by the Office of Naval Research through contract N00014-77-C-0354. In addition, we wish to thank R. S. Ault, J. M. Leech, and J. Woods for their many invaluable contributions to this project. Special thanks go to P. Blankinship for his meticulous preparation and deployment of instruments and moorings. He once again has taken our efforts to sea and provided a 100% mooring return. The crews of the Research Vessels *Researcher* (NOAA) and *Cape Hatteras* (UNC/Duke) performed expertly at sea. M. D. Jones has patiently endured the typing of several drafts of this manuscript with unfailing good humor.

APPENDIX A

Error Calculations

In this appendix, we derive the leading-order errors in the estimation of the mean value of some quantity from a stochastic series. The final formula, Eq. (A3), is quite simple to compute from the data, and is the formula we have used in our error analysis. Accordingly, we have made the implicit assumption that our errors are dominated by the uncertainties involved with the estimation of the means, rather than by, say, approximating derivatives by finite differences. This appears to be justifiable when describing the mean Gulf Stream.

Error in the mean. A consistent estimate of the mean of an ergodic time series is

$$\bar{x} = N^{-1} \sum_{j=1}^{N} x_j \qquad \text{(A1)}$$

where the overbar denotes the averaging operator and the subscripts denote particular elements of the time series. The question of the error in $\bar{x}$ concerns the quantity:

$$\sigma_{\bar{x}}^2 = \langle (\langle x \rangle - \bar{x})^2 \rangle \qquad \text{(A2)}$$

where the angle brackets denote an ensemble average. Expanding Eq. (A2) and using Eq. (A1) returns

$$\sigma_{\bar{x}}^2 = N^{-2} \sum_i \sum_j \langle x_i x_j \rangle - \langle x^2 \rangle.$$

The covariance term $\langle x_i x_j \rangle$ can be rewritten using

$$x_i = \langle x_i \rangle + x_i'$$

where the prime denotes a fluctuation about the mean, to give

$$\sigma_{\bar{x}}^2 = N^{-2} \sum_i \sum_j \langle x_i' x_j' \rangle.$$

If we assume that the time series is stationary, the fluctuation covariance, $\langle x_i' x_j' \rangle$, can depend only on $i - j$, in which case the above sum may be written as

$$\sigma_{\bar{x}}^2 = N^{-1} \sum_i R_i - N^{-2} \sum_i iR_i \qquad \text{(A3)}$$

where $R_k = \langle x_j' x_{j+k}' \rangle$. Equation (A3) applies to any average, (e.g., $\bar{u}$ or $\overline{u'v'}$) and has been used to compute the errors in our calculations.

The usual error measure, the standard error, is defined as

$$\sigma^2 = N^{-1} \times (\text{var}) = \langle x_i' x_i' \rangle / N.$$

Equation (A3) reduces to the above in the special case:

$$\langle x_i' x_j' \rangle = E\delta_{i,j}$$

where $\delta_{i,j}$ is the Kronecker delta function and E is the variance in the time series, which requires that the time series be white noise. It is doubtful if the DAMEX dataset—or any oceanographic dataset—meets this criterion. Further considerations of the sampling requirements necessary to measure eddy variability accurately are given by Flierl and McWilliams (1977).

REFERENCES

Bane, J. M., 1983: Initial observations of the subsurface structure and short-term variability of the seaward deflection of the Gulf Stream off Charleston, South Carolina. *J. Geophys. Res.*, **88**(C8), 4673–4684.

Bane, J. M., and D. A. Brooks, 1979: Gulf Stream meanders along the continental margin from the Florida Straits to Cape Hatteras. *Geophys. Res. Lett.*, **6**, 280–282.

——, D. A. Brooks and K. R. Lorenson, 1981: Synoptic observation of the three dimensional structure and propagation of Gulf Stream meanders along the Carolina continental margin. *J. Geophys. Res.*, **86**, 6411–6425.

——, and W. K. Dewar, 1983: The deflection and meander energetics experiment, current meter and bottom pressure gauge data report. University of North Carolina Tech. Rep. CMS-83-2.

——, and ——, 1986: Gulf Stream mean flow and variability near the Charleston bump. (in preparation)

Bevington, P. R., 1969: *Data Reduction and Error Analysis for the Physical Sciences*, McGraw-Hill, 336 pp.

Brooks, D. A. (Ed.), 1976: *Festa at NCSU*. Center for Marine and Coastal Studies, North Carolina State University.

——, and J. M. Bane, 1978: Gulf Stream deflection by a bottom feature off Charleston, South Carolina. *Science,* **201,** 1225–1226.

——, and ——, 1981: Gulf Stream fluctuations and meanders over the Onslow Bay upper continental slope. *J. Phys. Oceanogr.,* **11,** 247–256.

——, and ——, 1983: Gulf Stream meanders off North Carolina during winter and summer, 1979. *J. Geophys. Res.,* **88,** C8, 4633–4650.

Brooks, I. H., and P. P. Niiler, 1977: Energetics of the Florida Current. *J. Mar. Res.,* **35,** 163–191.

Bryden, H. L., 1983: Sources of eddy energy in the Gulf Stream recirculation region. *J. Mar. Res.,* **40,** 4, 1047–1068.

Chao, S. Y., and G. S. Janowitz, 1979: The effect of a localized topographic irregularity on the flow of a boundary current along the continental margin. *J. Phys. Oceanogr.,* **9,** 900–910.

Flierl, G. R., and J. C. McWilliams, 1977: On the sampling requirements for measuring moments of eddy variability. *J. Mar. Res.,* **35,** 797–820.

Fofonoff, N., 1954: Steady flow in a frictionless, homogeneous ocean. *J. Mar. Res.,* **13,** 254–263.

——, 1962: The dynamics of ocean currents. *The Sea; Ideas and Observations on Progress in the Study of the Seas, Vol. I.,* M. N. Hill, Ed., Wiley-Interscience, 3–30.

——, 1981: The Gulf Stream System. *Evolution in Physical Oceanography.* B. A. Warren and C. I. Wunsch, Eds., MIT Press, 112–129.

——, and M. M. Hall, 1983: Estimates of mass, momentum, and kinetic energy fluxes of the Gulf Stream. *J. Phys. Oceanogr.,* **13,** 1868–1877.

Halliwell, G. R., Jr., and C. N. K. Mooers, 1979: The space-time structure and variability of the shelf water-slope water and Gulf Stream surface front and associated warm core eddies. *J. Geophys. Res.,* **84,** 7707–7725.

Harrison, D. E., 1979: Eddies and the general circulation of numerical model gyres: An energetic perspective. *Rev. Geophys. Space Phys.,* **17,** 5, 969–979.

Hood, C. A., and J. M. Bane, 1983: Subsurface energetics of the Gulf Stream cyclonic frontal zone off Onslow Bay, North Carolina. *J. Geophys. Res.,* **88,** C8, 4651–4662.

Knauss, J. A., 1969: A note on the transport of the Gulf Stream. *Deep Sea Res.,* **16**(Suppl.), 117–123.

Lee, T. N., and L. P. Atkinson, 1983: Low frequency current and temperature variability from Gulf Stream frontal eddies and atmospheric forcing along the southeast U.S. outer continental shelf. *J. Geophys. Res.,* **88**(C8), 4651–4658.

——, and E. Waddell, 1983: On Gulf Stream variability and meanders over the Blake Plateau at 30°N. *J. Geophys. Res.,* **88**(C8), 4617–4632.

——, —— and R. V. Legeckis, 1981: Observations of a Gulf Stream frontal eddy on the Georgia continental shelf, April 1977. *Deep Sea Res.,* **28A,** 347–378.

Legeckis, R. V., 1979: Satellite observations of the influence of bottom topography on the seaward deflection of the Gulf Stream off Charleston, South Carolina. *J. Phys. Oceanogr.,* **9,** 483–497.

Luther, M. E., and J. M. Bane, 1985: Mixed instabilities in the Gulf Stream over the continental slope. *J. Phys. Oceanogr.,* **15,** 1, 3–23.

Maul, G. A., R. W. deWitt, A. Yanaway and S. R. Baig, 1978: Geostationary satellite observations of Gulf Stream meanders: Infrared measurements and time series analysis. *J. Geophys. Res.,* **83,** 6123–6135.

Munk, W. H., 1950: On the wind-driven ocean circulation. *J. Meteor.,* 7, 79–93.

Olson, D. B., O. B. Brown and S. R. Emmerson, 1983: Gulf Stream frontal statistics from Florida straits to Cape Hatteras derived from satellite and historical data. *J. Geophys. Res.,* **88,(C8),** 4569–4578.

Oort, A. H., 1964: Computations of the eddy heat and density transports across the Gulf Stream. *Tellus,* **16,** 55–63.

Pashinski, D. J., and G. A. Maul, 1973: Use of ocean temperature while coasting between the Straits of Florida and Cape Hatteras. *Mar. Wea. Log,* **17,** 1–3.

Pedlosky, J., 1979: *Geophysical Fluid Dynamics.* Springer-Verlag.

Pietrafesa, L. J., L. P. Atkinson and J. O. Blanton, 1978: Evidence for deflection of the Gulf Stream by the Charleston rise, *Gulfstream,* **4(9),** 3–7.

Rooney, D. M., G. S. Janowitz and L. J. Pietrafesa, 1978: A simple model of deflection of the Gulf Stream by the Charleston Rise. *Gulf Stream,* **4(11),** 3–7.

Schmitz, W. J., and P. P. Niiler, 1969: A note on the kinetic energy exchange between fluctuations and mean flow in the surface layer of the Florida Current. *Tellus,* **11,** 814–819.

Stommel, H. M., 1948: The westward intensification of wind-driven ocean currents. *Trans. Amer. Geophys. Union,* **29,** 202–206.

Sturges, W., 1974: Sea level slope along continental boundaries. *J. Geophys. Res.,* **79,** 6, 825–830.

Szabo, D., and G. L. Weatherly, 1979: Energetics of the Kuroshio south of Japan. *J. Mar. Res.,* **37,** 531–556.

Vukovich, F. M., and B. W. Crissman, 1980: Some aspects of Gulf Stream western boundary eddies from satellite and in-situ data. *J. Phys. Oceanogr.,* **10,** 1792–1813.

Webster, F., 1961a: The effect of meanders on the kinetic energy balance of the Gulf Stream. *Tellus,* **13,** 392–401.

——, 1961b: A description of Gulf Stream meanders off Onslow Bay. *Deep Sea Res.,* **8,** 130–143.

——, 1965: Measurements of eddy fluxes of momentum in the surface layer of the Gulf Stream. *Tellus,* **17,** 239–245.